arXiv:1409.3324v1 [cond-mat.mtrl-sci] 11 Sep 2014

Deformation behaviour of body centered cubic Fe nanowires under tensile and compressive loading

G. Sainath*, B.K. Choudhary and T. Jayakumar
Metallurgy and Materials Group
Indira Gandhi Centre for Atomic Research, Kalpakkam
Tamilnadu-603102, India

Abstract

Molecular Dynamics (MD) simulations have been carried out to investigate the deformation behaviour of <110> /{111} body centered cubic (BCC) Fe nanowires under tensile and compressive loading. An embedded atom method (EAM) potential was used to describe the interatomic interactions. The simulations were carried out at 10 K with a constant strain rate of $1 \times 10^8 s^{-1}$. The results indicate a significant differences in deformation mechanisms under tensile and compressive loading. Under tensile loading, the deformation occurs by the slip of full dislocations, While under compressive loading twinning was observed as the dominant mode of deformation. The tension-compression asymmetry in deformation mechanisms of BCC Fe nanowires is attributed to twinning-antitwinning asymmetry of 1/6<111> partial dislocation on {112} planes. We further explain the mechanism of dislocation pile up in tensile loading and twin growth in compressive loading.

Keywords: Molecular Dynamics; Nanowires; Tension; Compression; Slip; Twinning.
PACS : 83.10.Rs, 81.07.Gf, 62.20.M-, 61.72.Hh, 61.72.Mm

1 Introduction

Understanding the deformation behavior of nanscale materials has become a major interest for material scientists due to their potential applications in nano/micro electro-mechanical systems (NEMS/MEMS). BCC Fe nanowires with superior magnetic properties are useful in medical sensors, data-storage media, spin electronics and other memory devices [1, 2]. The complexities involved in performing experiments at nanoscale preclude the conventional testing methods and lend towards theoretical/computational tools. With the rapid progress of computational capability and the availability of reliable inter-atomic potentials, MD simulations have become a major tool to probe the mechanical behaviour of nanoscale materials. Moreover, MD simulations provide the atomistic detail of the deformation and damage mechanisms. In this work, atomistic simulations were utilized to investigate the mechanical behaviour of BCC Fe nanowires.

Many experimental and simulation studies have shown that the plastic deformation in nanoscale materials occurs through deformation twinning, dislocation slip and phase transformation [3, 4, 5]. The competition between these mechanisms mainly depends on crystallographic orientation, size and mode of loading (tension/compression). Particularly, with respect to mode of loading often an asymmetry is observed in deformation mechanisms of metallic nanowires. For example, the <100> oriented Au and Cu nanowires deforms by full dislocation slip under tensile loading, while partial dislocation slip is observed under compressive loading [3]. Similarly, the <110> oriented Au and Cu nanowires deforms by partial slip under tensile loading, while full slip is observed under compressive loading [3]. These results shows that the asym-

* email : sg@igcar.gov.in

metry in deformation mechanisms is orientation dependent. In face centered cubic (FCC) metals, slip occurs on {111} planes in <110> directions and the planar nature of the dislocation cores make the slip to follow the schmid's law and the asymmetry in deformation mechanisms can be attributed to different schmid factors for leading and trailing partial dislocations [3, 5]. In general, most of the studies in literature are mainly focused upon FCC metallic nanowires and comparatively few studies exist on their BCC counterparts [6, 7]. In BCC metals, the slip occurs in <111> direction along {110}, {112} and {123} planes and the non-planar nature of screw dislocations core makes the slip to violate the schmid's law. In Mo nanopillars, Kim et al.[6] studied the crystallographic orientation dependence of tension-compression asymmetry and shown that compressive flow stresses are higher than tensile ones in <100> orientation, and vice versa for <110> orientation. Healy and Ackland [7] had shown that the <100> oriented BCC Fe nanopillars deforms by twinning mechanism under tensile loading, while full dislocation slip is observed under compressive loading. However, it is not clear how the deformation mechanisms change with respect to mode of loading in other orientations, for example in <110> and <111> orientations. The present investigation is aimed to understand the deformation mechanisms under tensile and compressive loading of <110>/{111} BCC Fe nanowires using MD simulations.

2 Simulation details

Molecular Dynamics (MD) simulations have been carried out in Large scale Atomic/Molecular Massively Parallel Simulator (LAMMPS) package [8] employing an embedded atom method (EAM) potential for BCC Fe given by Mendelev and coworkers [9]. This potential was based on the framework of a Finnis-Sinclair (FS) type many body potential. The potential was fitted to the properties obtained using first-principles calculations in a model liquid configuration and also to other experimentally obtained material properties of BCC Fe.

Single crystal BCC Fe nanowire oriented in <110> axial direction with {111} as side surfaces were considered for this study. The nanowire had dimensions of $8.5 \times 8.5 \times 17\ nm^3$ ($30a \times 30a \times 60a$, where $a = 2.855\ A^0$ is lattice parameter of BCC Fe). The simulation box contains about 110000 Fe atoms arranged in BCC lattice. The nanowire length was set as twice the cross- section width (d) (aspect ratio 2:1). The fixed aspect ratio ensures, that the effects that are dependent on aspect ratio were eliminated. Periodic boundary conditions were chosen only along the wire axis, while the other directions were kept free in order to mimic an infinitely long nanowire. After initial construction of the nanowire, energy minimization was performed by conjugate gradient (CG) method to obtain a stable structure. The stable structure thus obtained is thermally equilibrated to a temperature of 10 K in canonical ensemble (constant NVT) by choosing the initial velocities of atoms randomly from a finite temperature Maxwell distribution. Velocity verlet algorithm was used to integrate the equation of motion with a time step of 5 fs.

Upon completion of the equilibration process, the tensile and compressive loadings were carried out at constant strain rate of $1 \times 10^8 s^{-1}$. The loading was applied along the nanowire axis (<110>). The strain rates considered here are very much higher than typical experimental strain rates due to the inherent timescale limitations from MD simulations. During the loading, the atomic system was allowed to deform naturally at constant strain rate, without imposing any stress constraints in other two directions. The strain is defined as $L - L_0/L_0$, where L is the current length of the nanowire and L_0 is the length just after the relaxation. The stress is calculated from the Virial expression of stress [10], which is equivalent to a Cauchy's stress in an average sense. Atom-Eye package [11] is used for visualization of atomic snapshots with centro-symmetry parameter (CSP) coloring [12]. The burger vector of a dislocations is determined by the Dislocation Extraction Algorithm (DXA) developed by Stukowski [13].

3 Results

Fig.1 shows the stress-strain curves of <110>/{111} BCC Fe nanowires under tensile and compressive loading upto 30% of strain at 10 K. In both loading conditions, initially the

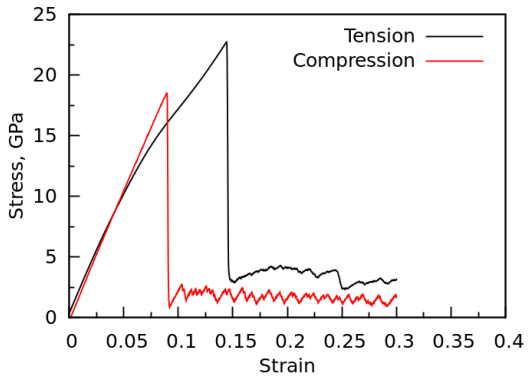

Figure 1: The stress-strain curves of <110>/{111} BCC Fe nanowires at 10 K under tensile and compressive loading

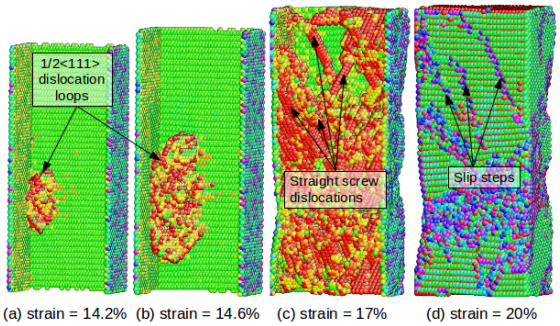

Figure 2: The atomic snapshots showing the deformation behaviour of <110>/{111} BCC Fe nanowires under tensile loading. (a) The nucleation (b) expansion of dislocation loops (c) accumalation of straight screw dislocations and (d) the slip steps formed due to dislocation escape. The atoms are colored according to the centro-symmetry parameter (CSP) [12]. The perfect BCC atoms and the front surfaces are removed for clarity in (a-c).

nanowires undergo an elastic deformation up to a peak stress, which can be designated as an yield strength of a defect-free nanowire. The Young's moduli obtained from the stress-strain curves was 200 GPa and it show no striking difference between the two loading conditions. Similarly, the magnitudes of the yield stress in tensile and compressive loadings were found to be 23 GPa and 18.5 GPa, respectively. The strength values are in close agreement with those obtained by ab-initio calculations for BCC Fe [14]. Following the peak, the flow stress drops abruptly to low values of stress, indicating the occurrence of yielding in the nanowires. It was observed that, the yielding under compressive loading occurred much earlier than in tensile loading. Further, it can be seen that, the magnitude of yield stress, flow stress and yield strain were higher in tensile than in compressive loading.

In order to understand the deformation behaviour under tensile and compressive loading, the evolution of atomic configurations at various strain levels were analysed using Atom-Eye package [11] with centro-symmetry parameter (CSP) coloring [12]. Fig. 2 shows the deformation behaviour under tensile loading of <110>/{111} BCC Fe nanowires at 10 K. It can be seen that the nanowire yields by the nucleation of collective dislocation loops from a single source at the corner of the nanowire (Fig. 2(a)). The DXA analysis indicates that, the dislocation loops had a screw character with burger vector of 1/2<111> (full dislocations). The yielding in the nanowire causes an abrupt drop in flow stress from a peak to a low level of stress. Previous studies on single crystal Fe-3%Si had shown that, once the stress reaches close to the theoretical strength, several dislocations loops might nucleate from the same source [15]. Since, there are no obstacles present in the nanowire, once nucleated avalanche of dislocations loops easily expand in multiple directions as shown in Fig. 2(b). With increasing deformation, the accumulation of large number of screw dislocations can be seen in Fig. 2(c). The pile-up of straight screw dislocations in BCC metals has been discussed previously by Groger and Vitek [16] with a mesoscopic model and Kaufmann et al. [17], using kinetic pile-up model. Experimentally Kim et al. [6], had shown that, when mixed dislocation loops are present in the sample during annealing, its edge components move and annihilate at a faster rate than the screw components. As a result, the screw dislocations likely remain in the metal, post annealing. The typical mechanism of screw dislocation accumulation in BCC Fe nanowires is shown in shown in Fig. 3. The dislocation loops initially emitted from the nanowire corner had a mixed character (Fig. 3(a)). With increasing strain, the expansion of dislocation loops associated with the decrease in the curvature can

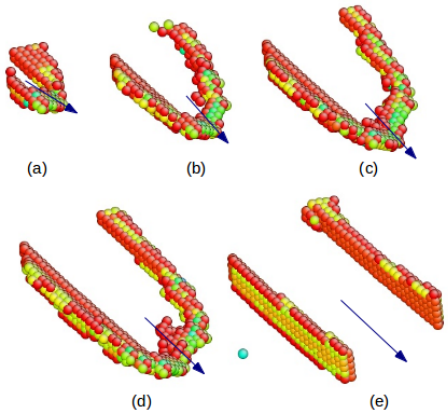

Figure 3: The typical mechanisms of straight screw dislocations pile-up in <110>/{111} BCC Fe nanowires under tensile loading. The atoms on dislocation cores are only shown. The blue arrow represents the burger vector direction

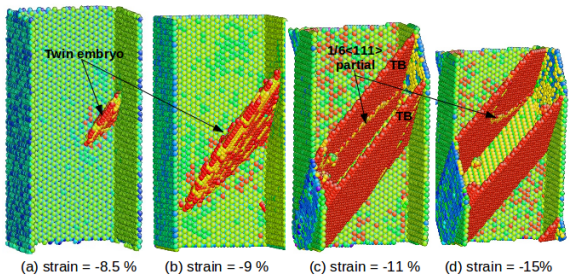

Figure 4: The atomic snapshots showing the deformation of <110>/{111} BCC Fe nanowires under compressive loading. (a) The nucleation (b) growth of twin embryo (c) forming a full twin plate and (d) twin growth. The atoms are coloured according to the centro-symmetry parameter (CSP) [12]. The perfect BCC atoms and front surfaces are removed for clarity.

be seen in Fig. 3(b-c). Since, edge dislocations in BCC metals have higher mobility than the screw dislocations, the edge component of mixed dislocations can easily reaches the surface (Fig. 3 (d) and (e)) and annihilates, leaving a well defined slip steps on the nanowire surface and many of such slip steps can be seen in Fig. 2(d). As a result of edge dislocation escape, only screw component of a dislocation loop remains in the nanowire (Fig. 3(e)).

Fig. 4 shows the atomic configurations at various stages of deformation during the compressive loading of <110>/{111} BCC Fe nanowires. It can be seen that the yielding under compressive loading occurs by the nucleation of a twin embryo from the corners of the nanowire (Fig. 4(a)), causing an abrupt drop in flow stress. The initially nucleated twin embryo propagate towards the other surface (Fig. 4(b)). The twin embryo consists of 1/6<111> partial dislocations along with 'twin' like stacking faults on {112} planes (Fig. 4(a-b)). With increasing strain, the leading edge of a twin embryo reaches the opposite surface and becomes full twin enclosed by twin boundaries on {112} planes as shown in Fig. 4(c). With further increase in deformation, the twin grows by the motion of twin boundary along the nanowire axis (Fig. 4(c-d)). The twin growth or twin boundary motion along the nanowire axis occurs by repeated initiation and glide of 1/6<111> twinning partial dislocations on adjacent {112} planes. It can be seen that, the high stress is required for the twin nucleation, but comparatively low stress is sufficient for twin growth or twin boundary motion. This is because the twin nucleation involves the creation of new fault area, where as the twin growth will not create any new fault area and therefore low energy is sufficient.

Fig. 5 shows the process of twin growth under the compressive loading of <110>/{111} BCC Fe nanowires. As shown in the Fig. 5, the twin boundary is of displaced type [22], consisting of two 1/12<111> dislocations lying in the adjacent {112} planes, marked 1 and 3 in Fig. 5(a). The 1/6<111> (= 1/12<111> + 1/12<111>) partial dislocations propagates further on {112} twin boundaries as shown in Fig. 5(b-c) and annihilates at the opposite surface (Fig. 5(d)). The splitting of 1/6<111> partial dislocation in BCC Fe is in agreement with the observation made by Yamaguchi et al. [22]. Again the next 1/6<111> twinning partial dislocation nucleates next to the first one (Fig. 5(e)), glides on the adjacent {112} plane (Fig. 5(f-g)) and again annihilates at the opposite surface. By repeating this process, the twin grows along the nanowire axis. Each nucleation and annihilation of twinning partial dislocation removes one interplaner spacing from the parent lattice and adds to twin lattice (In Fig. 5(a-d), the layer 3 is re-

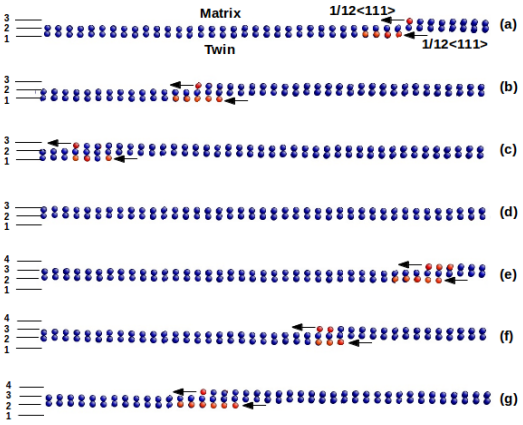

Figure 5: The process of twin growth in <110>/{111} BCC Fe nanowires under compressive loading. The twin growth proceeds by repeated initiation and glide of 1/6<111> (= 1/12<111> + 1/12<111>) partial dislocations on adjacent {112} planes. The blue atoms represents {112} twin boundary and arrow marks on twin boundary show the 1/12<111> partial dislocations. For clarity the twin boundary layers are marked with numerics 1,2,3 and 4

moved from the parent lattice and correspondingly the layer 1 is added to twinned lattice). This mechanism results the twin plate to thicken by a layer by layer growth process. The twin growth during the deformation results in a constant plateau observed in flow stress.

4 Discussion

The stress-strain behaviour of <110>/{111} BCC Fe nanowires had shown that the yield stress under tensile loading is higher than that of compressive loading. It indicates that the yield strength exhibits tension-compression asymmetry. Similar to the present results, many atomistic simulations studies on FCC and BCC metallic nanowires have shown an asymmetry in yield stress [6, 18, 19]. In FCC metallic nanowires it has been attributed to the presence of intrinsic stress in the nanowire caused by surface stress [19]. The present results show that, the tension-compression asymmetry in BCC Fe nanowires is mainly due to distinct differences in yielding mechanisms. Since the yield stress is associated with defect nucleation, the distinct yielding mechanisms leads to a tension-compression

Table 1: Deformation mechanisms

Loading type	Loading axis <110>	<100>
Tension	Dislocation slip*	Twinning [7]
Compression	Twinning *	Dislocation slip [7]

* present study

asymmetry in yield stress. Under tensile loading, the yielding occurs by the nucleation of high energy full dislocations (Fig. 2(a)), whereas in compression, it occurs by the nucleation of relatively low energy partial dislocations which causes twinning (Fig. 4(a)). Another factor influencing the tension-compression asymmetry of BCC Fe nanowires is related to the intrinsic properties of screw dislocations in BCC metals [6, 20]. The core of 1/2<111> screw dislocations in BCC metals spreads into several non-parallel planes of <111> zone [20]. As a result, the glide of a screw dislocation depends on the shear stress in slip direction along with the stress perpendicular to the slip direction, known as non-glide stress. The non glide stress is positive for tension, facilitating the easy glide and analogously it is negative for compression, making the dislocation glide difficult [21].

Table 1 summarizes the deformation mechanisms observed in <110>/{111} BCC Fe nanowires to that observed in <100>/{110} nanowires by Healy and Ackland [7]. Healy and Ackland [7] observed twinning under tensile loading and dislocation slip under compressive loading of <100>/{110} BCC Fe nanowires. It can be seen that the tension-compression asymmetry in deformation mechanisms of <110>/{111} BCC Fe nanowires is distinctly different than what has been observed in <100>/{110} BCC Fe nanowires. This is mainly because, the <100> and <110> orientations show a opposite twinning-antitwinning slip on {112} planes [6]. Under compressive loading of <110>/{111} BCC Fe nanowires, the 1/6<111> partial dislocation glides in twinning sense leading to the deformation by twinning. While in tension, it glides in antitwinning sense (opposite direction), making the dislocation glide more difficult on {112} planes. As a result, the dislocation may prefer to glide on secondary slip planes such as {110} or {123} leading to the deformation through slip in anti-twinning direction. This mechanisms

is reversed for <100>/{110} BCC Fe nanowires. Therefore, the observed tension-compression asymmetry in deformation behaviour of BCC Fe could be due the twinning-antitwinning asymmetry of 1/6<111> partial dislocation on {112} planes.

5 Conclusion

In summary, molecular dynamics simulations on <110>/{111} BCC Fe nanowires show that the deformation mechanisms vary with mode of loading. Under tensile loading, the deformation occurs by the full dislocations and the pile up of straight screw dislocations is observed. Whereas under compressive loading, the twinning was observed as predominant mode of deformation and the growth of twin occurred through the repeated initiation and glide of 1/6<111> (= 1/12<111> + 1/12<111>) partial dislocations on adjacent {112} planes. The twin boundary is found to be of displaced type, consisting of two 1/12<111> dislocations lying in the adjacent {112} planes. Due to distinct yielding mechanisms, the yield strength exhibited tension-compression asymmetry. The observed tension-compression asymmetry in deformation behaviour of BCC Fe nanowires is attributed the twinning-antitwinning asymmetry of 1/6<111> partial slip on {112} planes.

References

[1] X.Y. Zhang, G.H. Wen, Y.F. Chan, R.K. Zheng, X.X. Zhang and N. Wang, Fabrication and magnetic properties of ultrathin Fe nanowire arrays, Appl. Phys. Lett., 83, 3341-43 (2003)

[2] American elements, Iron Nano rods, http://www.americanelements.com/femnr.html

[3] H.S. Park, K. Gall and J.A. Zimmerman, Deformation of FCC nanowires by twinning and slip, J. Mech. Phys. Solids, 54, 1862-81 (2006)

[4] T. Zhu and J. Li, Ultra-strength materials, Prog. Mater. Scie., 55, 710-57 (2010)

[5] C.R. Weinberger and W. Cai, Plasticity of metal nanowires, J. Mater. Chem., 22, 3277-92 (2012)

[6] J.Y. Kim, D. Jang and J.R. Greer, Crystallographic orientation and size dependence of tension-compression asymmetry in molybdenum nano-pillars, Int. J. Plasticity, 28, 46-52 (2012)

[7] C.J. Healy and G.J. Ackland, Molecular dynamics simulations of compression-tension asymmetry in plasticity of Fe nanopillars, Acta Mater., 70, 105-112 (2014)

[8] S.J. Plimpton, Fast parallel algorithms for short-range molecular dynamics., J. Comput. Phys., 117, 1-19 (1995)

[9] M.I. Mendelev, S. Han, D.J. Srolovitz, G.J. Ackland, D.Y. Sun and M. Asta, Development of new inter-atomic potentials appropriate for crystalline and liquid iron. Philos. Mag., 83, 3977-94 (2003)

[10] Zimmerman J.A, Webb E.B, Hoyt J.J, Jones R.E, Klein P.A and Bammann D.J, Calculation of stress in atomistic simulation., Modell. Simul. Mater. Sci. Eng., 12, 319-32 (2003)

[11] J. Li, AtomEye: an efficient atomistic configuration viewer. Modell. Simul. Mater. Sci. Eng., 11, 173-77 (2003)

[12] C.L. Kelchner, S.J. Plimpton and J.C. Hamilton., Dislocation nucleation and defect structure during surface indentation., Phy. Rev. B, 58, 11085 (1998)

[13] A. Stukowski and K. Albe, Dislocation detection algorithm for atomistic simulations, Modell. Simul. Mater. Sci. Eng., 18, 025016 (2010)

[14] L. Yue-Lin, H. Rong-Jie, Z. Ying and L. Guang-Hong, Study of the theoretical tensile strength of Fe by a first-principles computational tensile test, Chin. Phys. B, 18,1923-08 (2009)

[15] L.Zhang and T.Ohmura, Plasticity Initiation and Evolution during Nanoindentation of an Iron–3% Silicon Crystal, Phys. Rev. Lett., 112, 145504 (2014)

[16] R. Groger and V. Vitek. Explanation of the discrepancy between the measured and atomistically calculated yield stresses in body-centred cubic metals. Philos. Mag. Lett., 87, 113-20 (2007)

[17] D. Kaufmann, R. Monig, C.A. Volkert and O. Kraft. Size dependent mechanical behavior of tantalum. Int. J. Plasticity, 27, 470-78 (2011)

[18] M.A. Tschopp and D.L. McDowell, Tension-Compression Asymmetry in Homogeneous Dislocation Nucleation in Single Crystal Copper, Appl. Phys. Lett., 90, 121916 (2007)

[19] J. Diao, K. Gall and M.L. Dunn, Yield Strength Asymmetry in Metal Nanowires, Nano Lett., 4, 1863-67 (2004)

[20] V. Vitek, Core structure of screw dislocations in body-centred cubic metals: relation to symmetry and interatomic bonding, Philos. Mag., 84, 415-28 (2004)

[21] J.Y. Kim and J.R. Greer, Tensile and compressive behavior of gold and molybdenum single crystals at the nano-scale, Acta Mater., 57, 5245-53 (2009)

[22] M. Yamaguchi and V. Vitek, Twin boundaries and incoherent steps on twin boundaries in body-centred-cubic metals, Philos. Mag., 34, 1-11 (1976)